ADVANCED FUNCTIONAL MATERIALS

# Mechanical and Structural Properties of $BaCrO_4$ Nanorod Films under Confinement and Shear**

By *Delphine Gourdon*,* *Mario Yasa*, *Anna R. Godfrey Alig*, *Youli Li*, *Cyrus R. Safinya*, and *Jacob N. Israelachvili*

Using an X-ray surface forces apparatus (X-SFA) we have investigated the effects of normal load (stress) and shear on the ordering and tribological properties of 10 nm × 30 nm surfactant-coated $BaCrO_4$ nanorods in isooctane, confined within submicrometer films. The film structure and corresponding friction forces were monitored as a function of time and shearing distance at different gap sizes and loads. The X-ray diffraction patterns indicate a cubic phase of nanorods coexisting with a surfactant phase that depends on the load, film thickness, shear rate, and shearing time. Atomic force microscopy and birefringence measurements performed on each surface after a shearing experiment showed ordered domains of nanorods over length scales of several tens of micrometers.

## 1. Introduction

Colloidal inorganic nanoparticles have size-dependent optical, optoelectronic, and material properties that are expected to lead to nanostructured materials with a wide range of practical applications.[1] The processing of such materials, and their potential use as lubricant additives, requires an understanding of how anisotropic nanoparticles order, both in terms of positioning and orientation, at surfaces or when confined within a thin film between two surfaces.[2,3] In this study, we have investigated the ordering and tribological properties of $BaCrO_4$ nanorod films under high confinement (high normal external load), shear, and rolling.

## 2. Results and Discussion

### 2.1. Characterization of Bulk $BaCrO_4$ Nanorod Suspensions

The nanorods were prepared as concentrated colloidal dispersions (suspensions) using published procedures.[4,5] The nanorods were covered with a monolayer of aerosol dioctylsulfosuccinate (AOT) surfactant molecules and dispersed in isooctane to make a stable suspension. Their size, uniformity, and bulk microstructure were checked using transmission electron microscopy (TEM). The samples were prepared by depositing a drop of the nanorod solution onto a Cu TEM grid coated with carbon/Formvar (polyvinyl formal). Figure 1a shows transient one-dimensional (linear) micelles present in the $BaCrO_4$ suspension, revealing nanorods 25–30 nm long. Figure 1b displays the final two-phase system: a concentrated two-dimensional cubic (oblique) phase of nanorods surrounded by a di-

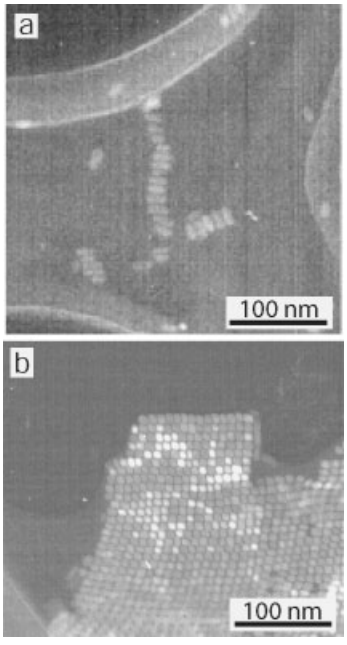


**Figure 1.** TEM images of $BaCrO_4$ nanorod superlattice structures in the bulk after a drop of the nanorods solution was deposited on a holey carbon grid (acceleration voltage: 200 kV). The nanorods are 8–10 nm wide (their section is slightly rectangular) and 25–30 nm long. a) Transient one-dimensional (linear) micelles of $BaCrO_4$ nanorods. b) Final two-phase system: a concentrated two-dimensional cubic (oblique) phase of nanorods, surrounded by a dilute phase (of AOT surfactants in isooctane).

[*] Dr. D. Gourdon,* A. R. Godfrey Alig, Dr. J. N. Israelachvili
Department of Chemical Engineering and Materials Research Laboratory
University of California at Santa Barbara
Santa Barbara, CA 93106 (USA)
E-mail: delph@engineering.ucsb.edu
M. Yasa, Dr. Y. Li, Dr. C. R. Safinya
Department of Materials and Materials Research Laboratory
University of California at Santa Barbara
Santa Barbara, CA 93106 (USA)

[**] This work was supported by the Office of Naval Research under Grant N00014-00-1-0214, and made use of Materials Research Laboratory Central Facilities supported by the MRSEC Program of the National Science Foundation under award No. DMR00-80034. The authors thank Dr. Yuval Golan for many useful discussions.

 © 2004 WILEY-VCH Verlag GmbH & Co. KGaA, Weinheim DOI: 10.1002/adfm.200305078 

lute phase of excess surfactant (AOT) molecules and isooctane. The nanorods were found to have a slightly rectangular section of 8 nm × 10 nm; these results confirm previous TEM characterizations.[5,6] We note also that the cubic phase mentioned above corresponds to the ordered phase detected in the small angle region of the X-ray diffraction spectrum of the confined nanorods (shown later).

### 2.2. Processing of $BaCrO_4$ Nanorod Films

We first carried out conventional surface forces apparatus (SFA) experiments, allowing us to image the confined and sheared films by observing the FECO (fringes of equal chromatic order), at the same time as normal and lateral (shear) forces were applied and measured. Figure 2 shows the fringe patterns recorded as two mica surfaces confining the nanorod suspension in isooctane were pressed together, when the applied load, $L$, was 24 mN (Fig. 2a) and ~135 mN (Fig. 2b).

In normal force measurements we found that the rods aggregate weakly to each other and that the aggregates adsorb to the surfaces. When the surfaces are pressed together, they show an initial long-range monotonic repulsion (range ~600 nm). Figure 3 displays the force profile recorded when the distance separating the surfaces is smaller than 200 nm, as well as schematics of the rods under confinement. At low load (and below 200 mN) the formation of discrete layers or 'terraces' is observed (consistent with the flat, vertical parts of the fringes in Fig. 2a, with heights of up to ~100 nm). At a higher load

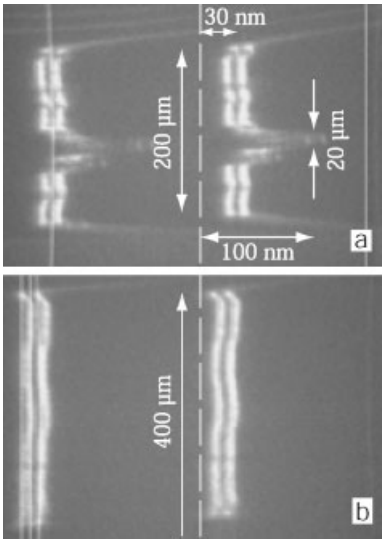


**Figure 2.** FECO images of confined $BaCrO_4$ nanorod films a) after being pressed together by a load of 24 mN. Apart from the flattened regions that show films of roughly uniform thickness (of 30 ± 5 nm), there are terraces (plateaus) up to 100 nm high and up to 20 μm wide. b) At higher loads (> 90 mN) and after some shear, the plateaus have collapsed, leaving only one fairly uniform terrace extending over the whole contact area (of diameter > 400 μm) and of thickness 1 or 1.5 nanorod diameters. The vertical dashed line corresponds to the position of the fringe when no $BaCrO_4$ film is confined (mica against mica), i.e., to the calibration of the 0 for our film thickness ($T$) measurements.

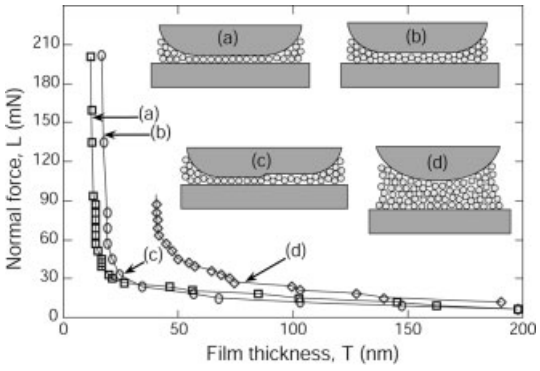


**Figure 3.** Normal force profile and schematics of the nanorods in solution under confinement. Below 200 nm, the formation of discrete layers or 'terraces' is observed (see inset diagrams c,d). "Hard walls" were found at 12.2 nm (a), and 16.4 nm (b), corresponding to 1 and 1.5 rod diameters, respectively.

($L > 90$ mN), and after some shearing and rolling of the two surfaces (due to the finite compliance of the supporting spring), the thick plateaus located on the edges of the contact have collapsed, leaving only one large terrace. If we assume that the hydrophilic confining mica surfaces are also covered by a monolayer of AOT from the solution, the thickness of this terrace or film is 1.0 or 1.5 nanorod diameters (see "hard walls" (a) and (b) at 12.2 nm and 16.4 nm). These results indicate that the rods are mostly aligned parallel to the surfaces. We note that the highest load (200 mN) corresponds to a pressure of only 2 MPa (~20 atm (1 atm = 101 325 Pa)) because of the large contact area, 0.12 $mm^2$, arising from the low stiffness of the glue used to mount the mica sheets to the cylindrical silica surfaces. Another important result is that no adhesion force was measured when the surfaces were pulled apart after compression.

It is important to note that pressure alone was not enough to induce the nanorods to order into such thin uniform films: some small back and forth shearing and rolling (or rocking) motion of the two surfaces relative to each other was also necessary to squeeze out the terraces. With pressure alone, the terraces (especially the ones trapped at the middle of the area of contact) remained in place as the mean contact area increased. The factors (optimum shear rate, shear amplitude, number of shear cycles, etc.) needed to produce such ordered nanofilms were not investigated in detail.

### 2.3. Tribology of $BaCrO_4$ Nanorod Films

One of our X-SFA studies was performed at the Stanford Synchrotron Radiation Facility, which allowed us to measure the ordering transition of the nanorods in the shearing film simultaneously with the friction forces in real time. This correlation is described in the following section; we first describe the results of the friction measurements. In this process, the surfaces were cycled back and forth at a constant sliding velocity $V$ over a fixed distance or 'amplitude' $A_0$. Both the friction forces and the film structure changed continuously with time


© 2004 WILEY-VCH Verlag GmbH & Co. KGaA, Weinheim

over many hours after the commencement of sliding, and even after 10 h of continuous shearing steady-state conditions had not been fully attained.

Figure 4a shows the results of a series of tribological experiments done at different gaps of confinement $T$ of the nanorod film. During the whole series, both the shearing (sliding) velocity $V$ and the shearing amplitude $A_0$ were kept constant, 5.5 μm s$^{-1}$ and 30 μm respectively. The film thickness was progressively reduced from 30 μm (corresponding to a normal force $L \approx 9$ mN) to less than 1 μm (corresponding to $L > 17$ mN) and the friction force was recorded versus time of shearing. As expected, the friction forces increase with increasing $L$ and decreasing $T$. Note also that for $T < 1$ μm (the smallest gap investigated) the friction force—rather than evolving smoothly—exhibits an initial drop at $t = 0$ and again at $t = 10$ min before it increases slowly to its steady-state value. This indicates that at the smallest gap, freshly created junctions such as the terraces described in Figures 2,3 are probably broken as the surfaces slide past each other. Part of the rods forming the terraces are then squeezed out of the contacting region, while the other ones are forced to redistribute (in terms of positioning) and rearrange (in terms of orientation) within the shearing junction, leading to a higher friction force and also a longer time to reach steady-state conditions (> 120 min).

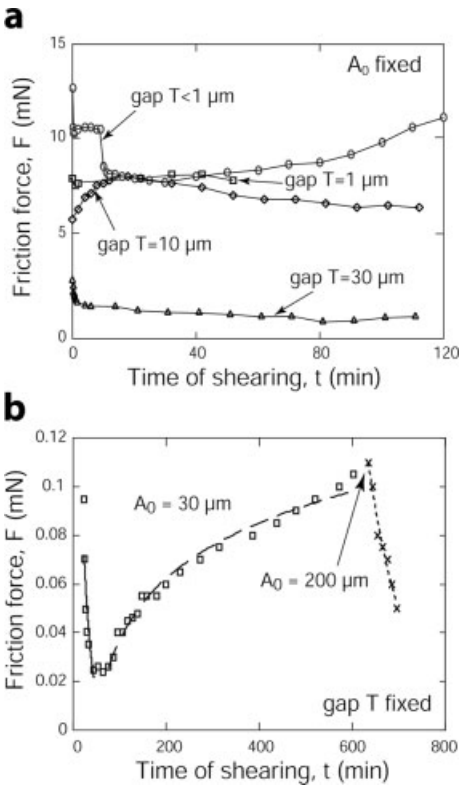


**Figure 4.** a) Friction force versus shearing time of the nanorod film at different gaps $T$ of confinement and applied loads $L$ ($L$ ranges from 9 mN when $T = 30$ μm to > 17 mN when $T < 1$ μm). The shearing velocity was kept constant at $V = 5.5$ μm s$^{-1}$, as well as the shearing amplitude $A_0$ (30 μm). b) Friction force versus shearing time of a thicker nanorod film ($T = 80$ μm). At $t = 570$ min, the shearing amplitude $A_0$ was raised from 30 μm to 200 μm, while the actual sliding velocity was kept constant (by decreasing the scanning frequency).

Figure 4b shows the friction force versus shearing time at a sliding (shearing) velocity of $V = 5.5$ μm s$^{-1}$, and a load of $L \approx 1.5$ mN, where the film thickness was $T \approx 80$ μm. At this large gap the friction was naturally very small but already detectable. The initial decay of the friction force with shearing time, $F(t)$, was exponential (see solid-line fit). However, soon after the initial drop in $F$, the friction force increased slowly in a roughly logarithmic fashion (see dashed line fit), i.e., without leveling off or reaching steady-state conditions, even after 10 h of shearing. Figure 4b also shows what happens when the shearing amplitude $A_0$ is changed. At $t \approx 10$ h, $A_0$ was raised from 30 μm to 200 μm (keeping the same $V$), which caused new (previously untouched) surfaces to be sheared. As could have been expected, this increase in $A_0$ was followed by a rapid drop in the friction force with time, very similar to the initial drop of freshly created films. The relaxation times of these initial drops are of the order of minutes. These are much shorter than the hours needed to attain steady-state conditions, but still significantly longer than the natural frequency (~ 0.02 s) of the friction-force-measuring spring. Thus, the friction measurements allow us to identify at least two distinct relaxation times, which are presumably determined by some dynamic property or properties of the shearing film (other than the inertia of the system). However, since all the measurements were done at the same $V$, it is also possible that the total or cumulative distance sheared is the 'characteristic' parameter of the system, rather than the shearing time.[7,8]

In a separate SFA experiment (results not shown here) we found that the friction force at constant shearing amplitude $A_0$ was nearly independent of sliding velocity over a range of four decades from 1 nm s$^{-1}$ to 10 μm s$^{-1}$. These results reinforce the idea that the actual sliding velocity is not a critical parameter in the tribological process. Finally, we also observed that the friction force followed Amontons' law, i.e., the friction force $F$ increased linearly with the applied load $L$ ($F = \mu L$, where $\mu = 0.90 \pm 0.15$). This intriguing behavior has been observed experimentally on a wide variety of non-adhesive systems[9] (rough and smooth), ranging from the macro to the nanoscale, and has been recently predicted by molecular dynamics simulations.[9]

### 2.4. Ordering of the $BaCrO_4$ Nanorods under Confinement and Shear

X-SFA measurements were also made at the University of California, Santa Barbara (UCSB) using a standard beamline. These measurements allowed us to monitor the slow ordering of the $BaCrO_4$ nanorods with time as they were sheared under confinement. Typically, the nanorod suspension was injected between the surfaces separated by a gap of 500 μm, after which the surfaces were slowly pressed together. Figure 5a displays time-resolved X-ray scans recorded both in static conditions (at several gaps) and during shearing at $V = 5.5$ μm s$^{-1}$, when

 © 2004 WILEY-VCH Verlag GmbH & Co. KGaA, Weinheim 

ADVANCED FUNCTIONAL MATERIALS



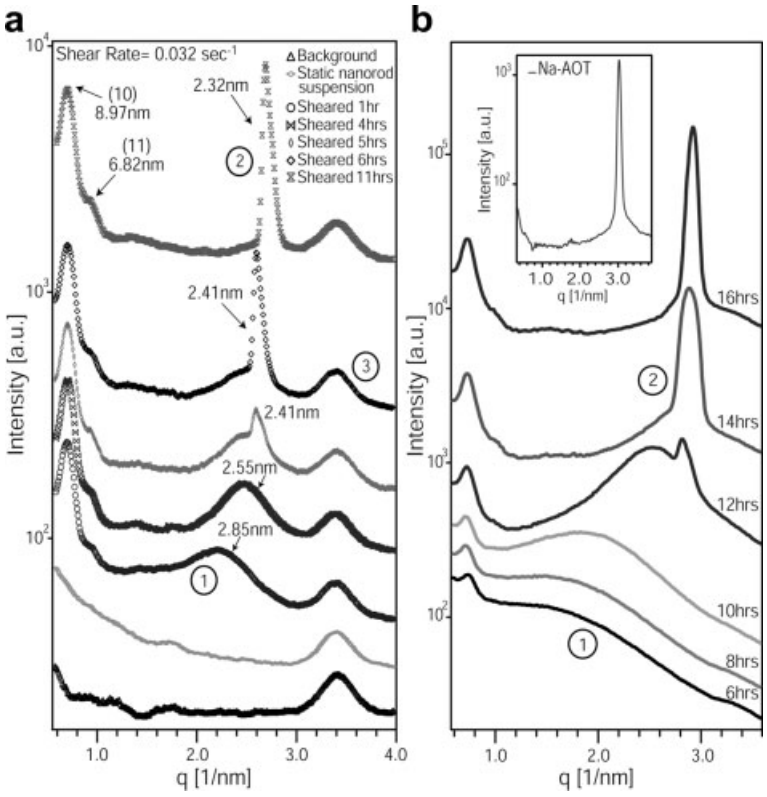


**Figure 5.** a) Time evolution of the diffraction spectrum of a confined $BaCrO_4$ nanorod suspension undergoing continuous shear (gap width or film thickness: $T = 170$ μm, shear rate: $V/T = 0.032$ $s^{-1}$). During shearing the small-angle region indicates progressive ordering of the nanorods from an initially disordered structure into a cubic (oblique) structure. Also, a broad (ordered liquid phase) Bragg peak (Peak 1) appears at $q = 2.20$ $nm^{-1}$ ($d$-spacing = 2.85 nm) that gradually shifts to a smaller $d$-spacing. After 5 h of shear, an additional narrow (ordered crystalline phase) peak (Peak 2) appears at $q = 2.61$ $nm^{-1}$ ($d$-spacing = 2.41 nm). b) Time evolution of the diffraction spectrum of a bulk $BaCrO_4$ nanorod suspension in a quartz capillary. As the solvent (isooctane) evaporates, the structure formed by the $BaCrO_4$ nanorods is fixed (peak at $q = 0.70$ $nm^{-1}$), and crystallization of excess AOT occurs (illustrated by the transition from a broad to a sharp peak at large $q$). The curves are offset along the $y$-axis for clarity. Inset: X-ray data taken in dry Na-AOT surfactant (not dissolved in any solvent).

the film thickness was about $T = 170$ μm (shear rate $V/T = 0.032$ $s^{-1}$) and the shearing amplitude $A_0$ was 30 μm. For clarity, the curves are offset along the $y$-axis. No Bragg peak was observed under static conditions. However, a crystallization process was readily observed as soon as shearing started: the small angle region of the X-ray diffraction spectrum shows a high intensity Bragg peak at $q = 0.70$ $nm^{-1}$ ($d$-spacing = 8.97 nm) and a shoulder at $q = 0.92$ $nm^{-1}$ ($d$-spacing = 6.82 nm) that indicate ordering of the nanorods into the cubic (oblique) structure shown in Figure 1b. Also, as shear progresses a broad Bragg peak (Peak 1), (most likely an ordered liquid nematic phase, appears at $q = 2.20$ $nm^{-1}$ ($d$-spacing = 2.85 nm) that gradually shifts to higher $q$ values (smaller $d$-spacing). After 5 h of shear, an additional narrow peak (Peak 2) appears at $q = 2.61$ $nm^{-1}$ ($d$-spacing = 2.41 nm) corresponding to a crystalline phase. From this point, the intensity of Peak 1 decreases while that of Peak 2 increases and shifts to higher $q$ values ($q = 2.70$ $nm^{-1}$, $d$-spacing = 2.32 nm). The peak observed at $q = 3.41$ $nm^{-1}$ (Peak 3) arises from a kapton window in the front X-ray flight path.

Experiments were also carried out with a bulk $BaCrO_4$ nanorod suspension. A small volume of the solution was transferred to a quartz capillary with an inner diameter of 1.5 mm. The capillary was left unsealed and exposed to air, which simultaneously allows the isooctane to evaporate quickly (much faster than in the X-SFA experiment, which is performed in a sealed chamber) and, eventually, water from the ambient air to penetrate the suspension. Figure 5b shows the evolution of the nanorod solution as the solvent is allowed to evaporate over a period of 20 h, during which time the suspension became increasingly more concentrated. After 6 h, we observe the same small angle peaks at $q = 0.72$ $nm^{-1}$ and $q = 1.00$ $nm^{-1}$ that develop during the X-SFA experiment (Fig. 5a), corresponding to the cubic structure formed by the rods. However the peak developing at $q = 1.50$ $nm^{-1}$ is much broader, and shifts much more gradually than in the SFA shearing experiments to the sharp peak at $q = 2.95$ $nm^{-1}$ that corresponds to a crystalline phase. To check the origin of this crystalline phase, a sample of dry AOT (the surfactant molecule used to stabilize the rods) was analyzed in a similar capillary. The results (Fig. 5b inset) show a peak at $q = 3.00$ $nm^{-1}$. The small difference observed with respect to the nanorod solution is most likely due to remaining isooctane that did not fully evaporate from the solution.

Unfortunately, our results do not allow us to make an unambiguous statement on the correlation between and relative importance of the nanorod and surfactant phases we observe in ultra-thin films subjected to a normal load and shear. Thus, they suggest that the structure of the nanorod and surfactant phases remain largely unaffected, but that their relative amounts differ.

### 2.5. Further Characterization of Nanorod Films after Confinement and Shearing

A further characterization of the $BaCrO_4$ nanorods was performed after a confinement and shearing experiment, using atomic force microscopy (AFM) and polarized light optical microscopy. Figure 6a shows an AFM image of one of the two mica surfaces used to confine and shear the nanorods after the solvent had been allowed to fully evaporate. A 50 nm high terrace can be seen extending over 10–20 μm. The terrace is only 35 nm high on the right edge. Both heights are consistent with the plateaus visualized under confinement in the SFA–FECO

 © 2004 WILEY-VCH Verlag GmbH & Co. KGaA, Weinheim 

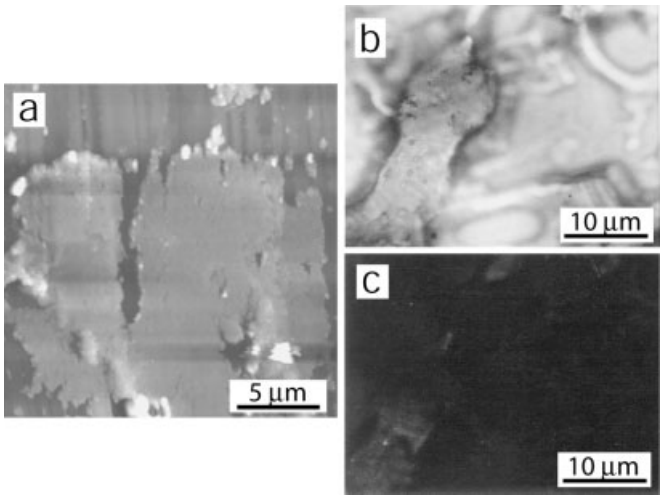


**Figure 6.** a) AFM image of mica coated with $BaCrO_4$ nanorods in isooctane where ~ 50 nm high terraces can be seen extending 10–20 µm, similar to what is 'seen' in the SFA-FECO experiments (Figs. 2,3). b) Polarized light optical microscopy of the X-SFA disks following the shearing experiment, without crossed-polarizers. c) As for (b), but with crossed polarizers. Birefringent domains, on a length-scale of several tens of micrometers, can be seen inside the zone that was previously the contact and sheared region.

experiments (Figs. 2,3). In addition, polarized light optical microscopy was performed on the same surfaces and the measurements (Figs 6b,c) showed birefringent (ordered) domains over length scales of several tens of micrometers. Thus, there appear to be several levels of 'hierarchical' structuring in this fascinating system, starting from the angstrom (nano) level and ranging to the sub-millimeter (macro) size regime. Future research under both static and dynamic (shearing, rolling) conditions should allow determination of the optimal experimental conditions for obtaining highly ordered nanostructured films of $BaCrO_4$ and other types of nanorods.

## 3. Conclusions

We have used the surface forces apparatus to characterize the normal and lateral (shear) forces of BaCrO4 nanoparticles (dispersed in isooctane) under confinement, and especially as a tool for processing (via rolling/shearing) monomolecular films of nanoparticles extending over large areas ($> 0.1$ mm$^2$). Our results suggest that the structure of nanorod and surfactant phases remain largely unchanged in confined films under a load and shear, but that their relative amounts differ.

## 4. Experimental

*SFA/MBI*: A surface forces apparatus (SFA), when modified for shear studies, allows for two contacting surfaces to be slid past each other at different driving velocities $V$ while simultaneously measuring the applied load $L$ and friction forces $F$ [10,11]. Back-silvered, atomically smooth mica surfaces were the primary surfaces used to confine the nanorod suspension under study. They were glued onto cylindrically curved silica disks, and placed in the sealed SFA with their axes perpendicular to each other, before a droplet of the solution was injected between them. As in previous SFA experiments, the surfaces were visualized optically with multiple beam interferometry (MBI) using 'fringes of equal chromatic order' (FECO), that allow the surface shape, contact radius $r$, area $A = \pi r^2$ and film thickness $T$ to be measured (the latter to an accuracy of 2 Å) either under quiescent conditions or during sliding [12].

*X-SFA*: A custom SAXS (small-angle X-ray scattering) beamline was used for all X-ray experiments. For in house experiments a Rigaku rotating anode X-ray generator (CuKa, 8 KeV) coupled with Osmic confocal optics was used to define an incident beam (0.8 mm × 0.8 mm at the sample position). A Marresearch Image plate was used to collect the diffracted X-ray beam (in house and at the Stanford Synchrotron Radiation Laboratory) 719 mm from the sample position. The geometry of the contacting surfaces with respect to the X-ray beam as well as other details concerning the experimental setup are reported in reference [13].

*TEM, Polarized Light Microscopy, AFM*: The electron micrographs were obtained on a JEOL 100 cx machine at an accelerating voltage of 100 kV. Polarized microscopy was performed on a Nikon Optiphot2-Pol microscope. The atomic force micrograph was obtained using a Veeco Dimension 3100 AFM operating in tapping mode at a scan rate of 1 Hz, with a pyramidal silicon nitride tip ($R = 30$ nm) mounted on a stiff cantilever.

Received: October 7, 2003
Final version: December 5, 2003

[1] C. Petit, A. Taleb, M. P. Pileni, *Adv. Mater.* **1998**, *10*, 259.
[2] L. Rapoport, Y. Bilik, Y. Feldman, M. Homyonfer, S. R. Cohen, R. Tenne, *Nature* **1997**, *387*, 791.
[3] L. Rapoport, Y. Feldman, M. Homyonfer, H. Cohen, J. Sloan, J. L. Hutchinson, R. Tenne, *Wear* **1999**, *229*, 975.
[4] J. D. Hopwood, S. Mann, *Chem. Mater.* **1997**, *9*, 1819.
[5] M. Li, H. Schnablegger, S. Mann, *Nature* **1999**, *402*, 393.
[6] F. Kim, S. Kwan, J. Akana, P. Yang, *J. Am. Chem. Soc.* **2001**, *123*, 4360.
[7] C. Drummond, J. N. Israelachvili, *Phys. Rev. E* **2001**, *63*, 041 506.
[8] D. Gourdon, J. N. Israelachvili, *Phys. Rev. E* **2003**, *68*, 021 602.
[9] J. Gao, W. D. Luedtke, D. Gourdon, M. Ruths, J. N. Israelachvili, U. Landman, *J. Phys. Chem. B*, in press.
[10] a) J. N. Israelachvili, G. E. Adams, *J. Chem. Soc., Faraday Trans. 1* **1978**, *74*, 975. b) S. Granick, *Science* **1991**, *253*, 1374. c) E. Kumacheva, J. Klein, *J. Chem. Phys.* **1998**, *108*, 7010.
[11] G. Luengo, F. J. Schmitt, R. Hill, J. N. Israelachvili, *Macromolecules* **1997**, *30*, 2482.
[12] a) J. N. Israelachvili, *J. Colloid Interface Sci.* **1973**, *44*, 259. b) M. Heuberger, G. Luengo, J. N. Israelachvili, *Langmuir* **1997**, *13*, 3839.
[13] Y. Golan, M. Seitz, C. Luo, A. Martin-Herranz, M. Yasa, Y. Li, C. R. Safinya, J. N. Israelachvili, *Rev. Sci. Instrum.* **2002**, *73*, 2486.

 © 2004 WILEY-VCH Verlag GmbH & Co. KGaA, Weinheim 